GENERALIZED LEAST SQUARES MULTIPLE 3D SURFACE MATCHING

Devrim Akca * and Armin Gruen

Institute of Geodesy and Photogrammetry, ETH Zurich, Wolfgang-Pauli-Str. 15, CH-8093 Zurich, Switzerland
(akca, agruen)@geod.baug.ethz.ch

Commission V, WG V/3

KEY WORDS: Surface matching, co-registration, multiple surfaces, 3D surface, pointcloud, georeferencing.

ABSTRACT:

A method for the simultaneous co-registration and georeferencing of multiple 3D pointclouds and associated intensity information is proposed. It is a generalization of the 3D surface matching problem. The simultaneous co-registration provides for a strict solution to the problem, as opposed to sequential pairwise registration. The problem is formulated as the Least Squares matching of overlapping 3D surfaces. The parameters of 3D transformations of multiple surfaces are simultaneously estimated, using the Generalized Gauss-Markoff model, minimizing the sum of squares of the Euclidean distances among the surfaces. An observation equation is written for each surface-to-surface correspondence. Each overlapping surface pair contributes a group of observation equations to the design matrix. The parameters are introduced into the system as stochastic variables, as a second type of (fictitious) observations. This extension allows to control the estimated parameters. Intensity information is introduced into the system in the form of quasisurfaces as the third type of observations. Reference points, defining an external (object) coordinate system, which are imaged in additional intensity images, or can be located in the pointcloud, serve as the fourth type of observations. They transform the whole block of "models" to a unique reference system. Furthermore, the given coordinate values of the control points are treated as observations. This gives the fifth type of observations. The total system is solved by applying the Least Squares technique, provided that sufficiently good initial values for the transformation parameters are given. This method can be applied to data sets generated from aerial as well as terrestrial laser scanning or other pointcloud generating methods.

1. INTRODUCTION

The early approach for the multiple pointclouds registration is to sequentially apply pairwise registrations until all views are combined. Chen and Medioni (1992) propose a method, which registers successive views incrementally with enough overlapping area. Each next view is registered and merged with the topological union of the former pairwise registrations. Later, this approach is equipped with a coarse-to-fine mesh hierarchy (Turk and Levoy, 1994), and the least median of squares (LMS or LMedS) estimator with random sampling (Masuda and Yokoya, 1995).

The shortcomings of the incremental solution were recognized early. The registration of a view does not change once it has been added to the integrated model. However, it is possible that a following view brings information that could have improved the registration of previously processed views (Bergevin et al., 1996; Pulli, 1999). Bergevin et al. (1996) propose a solution in which every view is sequentially matched with all other overlapping views. The procedure is iteratively executed over all views. The iteration is stopped when the registration converges. For each view a separate transformation is calculated, and they are applied simultaneously before the next run of iteration. Although it diffuses the registration errors evenly among all views, slow convergence is the main disadvantage. Benjemaa and Schmitt (1997) accelerate the method by applying the new transformation as soon as it is calculated (like the Gauss-Seidel method) and employ a multi-*z*-buffer technique which provides a 3D space partitioning. Pulli's (1999) solution performs pairwise registrations between every overlapping view pairs. Subsequently, these pairwise registrations are incrementally treated as constraints in a global registration step. However, these constraints do not imply functional constraints in the optimization scheme. Rather, it is a set of virtual points that uniformly subsample the overlapping areas, called as virtual mate. This approach has the capability to handle large data sets, since using the virtual mates from pairwise alignments does not require loading the entire data set into memory. A concrete mate version of this method, in which a set of corresponding points themselves rather than the virtual points is used as constraint, is proposed for robot navigation (Lu and Milios, 1997). The subsequent global registration is achieved by employing a sequential estimation procedure.

Alternatively, some works carry out the multiview registration task in the sensor coordinate system. In Blais and Levine (1995) couples of images are incrementally registered. It is based on reversing the range finder calibration process, resulting in a set of equations which can be used to directly compute the location of a point in a range image corresponding to an arbitrary location in the three dimensional space. Another multiview registration method based on inverse calibration, developed independently, called Iterative Parametric Point (IPP), is given in Jokinen (1998). Differently, it simultaneously registers all views using the Levenberg-Marquardt non-linear optimization technique. Although the reverse calibration method, also called point-to-projection technique, provides fast access mechanisms for the point correspondence, it is performed on 2.5D range maps. It is not suitable for truly 3D applications.

* Corresponding author. www.photogrammetry.ethz.ch

Stoddart and Hilton (1996) first find the pairwise correspondences between all the overlapping views, and then iteratively solve the global registration using a gradient descent algorithm. Although this is a two steps procedure, the final transformations are simultaneously computed as one system in the global registration step. A similar approach, developed independently, is given in Eggert et al. (1998). Neugebauer (1997) reduces the problem to only a global registration step, and simultaneously registers all views using the Levenberg-Marquardt method. Correspondence search is performed on the range maps, which is a 2.5D approach. Williams et al. (1999) suggest a further simultaneous solution by including a priori covariance matrices for each individual point. The non-linear system is solved using the Lagrange multipliers method, or so called Gauss-Helmert estimation model.

Iterative linear (closed-form) solutions have become very attractive. Although they are straightforward to implement, their stochastic model is of limited value in comparison to non-linear optimization techniques. Williams and Bennamoun (2001) present a generalization of Arun et al.'s (1987) well known pairwise registration method, which uses the Singular Value Decomposition (SVD) to compute the optimal registration parameters in the presence of point correspondences. This method is a closed-form solution for 3D similarity transformation between two 3D point sets. Beinat and Crosilla (2001) propose the Generalized Procrustes Analysis as a solution for the multiple range image registration problem in the presence of point correspondence. The Procrustes Analysis is another kind of closed-form solution, which was introduced by Schoenemann and Carroll (1970). In fact, both of the methods use Gauss-Seidel or Jacobi type of iteration techniques. Further similar methods are given in Sharp et al. (2004) and in Krishnan et al. (2005).

Recently, Al-Manasir and Fraser (2006) propose an alternative technique, called image-based registration (IBR), for digital camera mounted/integrated terrestrial laserscanner systems, based on the photogrammetric image orientation procedure. The network of images is first oriented using the bundle block adjustment, and then the exterior orientations are transferred to the laserscanner stations provided that the camera calibration and spatial relationship between the camera and laserscanner coordinate systems are known. Since it exclusively uses the imagery, registration can be achieved even in the situations where there is no overlap between the point clouds. However, the method is only applicable for camera mounted laserscanner data.

Several review and comparison studies are available in the literature (Jokinen and Haggren, 1998; Williams et al., 1999; Cunnington and Stoddart, 1999; Campbell and Flynn, 2001).

In a previous work, we proposed an algorithm for the least squares matching of overlapping 3D surfaces, called least squares 3D surface matching (LS3D). The LS3D method estimates the transformation parameters of one or more fully 3D search surfaces with respect to a template one, using the Generalized Gauss-Markoff model, minimizing the sum of squares of the Euclidean distances between the surfaces (Gruen and Akca, 2005). The mathematical model is a generalization of the Least Squares image matching method, in particular the method given by Gruen (1985).

In order to optimize the run-time, a rapid method for searching the correspondence is added. It is a space partitioning method, called 3D boxing (Akca and Gruen, 2005b). False correspondences with respect to outliers and occlusions are detected and eliminated using a weighting scheme adapted from Robust Estimation methods (Akca and Gruen, 2005c).

When the object surface lacks sufficient geometric information, i.e. homogeneity or isotropicity of curvatures, the basic algorithm will either fail or find a side minimum. We propose an extension of the basic algorithm in which available attribute information, e.g. intensity, color, temperature, etc., is used to form quasisurfaces in addition to the actual ones. The matching is performed by simultaneous use of surface geometry and attribute information under a combined estimation model (Akca and Gruen, 2005a).

When more than two pointclouds with multiple overlaps exist, we adopt a two step solution (Akca and Gruen, 2005b). First, pairwise LS3D matchings are run on every overlapping pairs and a subset of point correspondences are saved to separate files, similar to Lu and Milios's approach (1997). In the global registration step, all these files are passed to a block adjustment by independent models procedure (Ackermann et al., 1973), which is a well known orientation procedure in photogrammetry.

In some applications georeferencing is needed, which is the procedure to transform the spatial data from a local system to an external object coordinate system. We also provide for an integrated solution for this problem.

1.1 Our proposed method

Terrestrial laser scanning companies (e.g. Z+F, Leica, Riegl) commonly use special kind of targets for the registration of point clouds. However such a strategy has several deficiencies with respect to fieldwork time, personnel, equipment costs, and accuracy. In a recent study, Sternberg et al. (2004) reported that registration and geodetic measurement parts comprise 10-20% of the whole project time. In another study a collapsed 1000-car parking garage was documented in order to assess the damage and structural soundness of the structure. The scanning took 3 days, while the conventional survey of the control points required 2 days (Greaves, 2005). In a recent project conducted by our group at Pinchango Alto (Peru) two persons set the targets to the field and measured with Real-Time Kinematic GPS in 1½ days.

Not only fieldwork time but also accuracy is another important concern. The target-based registration methods cannot exploit the full accuracy potential of the data. The geodetic measurement naturally introduces some errors, which might exceed the internal error of the scanner instrument. In addition, the targets must be kept stable during the whole scanning campaign. This might be inconvenient with the scanning works stretching over more than one day. On the other hand, target-based registration techniques can provide immediate georeferencing to an object coordinate system.

Surface-based registration techniques stand as efficient and versatile alternative to the target-based techniques. They simply bring the strenuous additional fieldwork of the registration task to the computer in the office while optimizing the project cost and duration and achieving a better accuracy. However, they do not provide the georeferencing option.

This work proposes a method which combines the advantageous parts of both techniques based on the least squares matching framework. The proposed method is a (truly) simultaneous one step solution for the matching and georeferencing of multiple 3D surfaces with their intensity information. The mathematical model is a hybrid system which contains different type of observations. The proposed method is an algorithmic extension of our previous work given in Gruen and Akca (2005). It generalizes the 3D surface matching problem in the sense that multiple 3D surfaces with their intensity information are globally matched and simultaneously georeferenced. Multiple primitives, surface information (geometry and intensity) and the (reference) point features, are co-registered together.

The paper is structured as follow. The next chapter introduces the mathematical model with the execution aspects. The third chapter presents the experimental results.

2. MATHEMATICAL MODELLING

2.1 Least Squares Multiple 3D Surface Matching

Assume a set of n surfaces of an object: $g_1(x, y, z)$,…, $g_n(x, y, z)$. The object is defined in a 3D Cartesian coordinate system, whereas the n surfaces are located in arbitrary local coordinate systems. The n surfaces are discrete 3D approximations of continuous functions of the object surface. They are digitized according to a sampling principle.

The surface representation is carried out in a piecewise form, individually for each surface. $g_i(x, y, z)$ stands for any element of the i-th surface in this representation.

There are m mutual spatial overlaps between the surfaces $g_i(x, y, z)$. Every overlap satisfies a pairwise matching:

$$g_i(x,y,z) - e_i(x,y,z) = g_j(x,y,z) \quad , \quad i,j = 1,...,n \quad , \quad i \neq j \qquad (1)$$

where $e_i(x, y, z)$ is a true error vector. It is assumed that i-th surface's noise is independent of j-th one.

In order to prevent duplication, Equations (1) are written for every possible i-j pair with $i<j$.

Equations (1) are considered as nonlinear observation equations which model the observation vector $g_i(x, y, z)$ with functions $g_j(x, y, z)$. The Least Squares matching of the j-th surface to the i-th one is to be satisfied while the i-th surface is also subject to a 3D transformation (with respect to a predefined datum). This is the 3D analogy of the X-Y constraint version (i.e. grid sampling mode) of the multiphoto geometrically constrained matching (MPGC) (Gruen and Baltsavias, 1987) where both the template and the search image patches are transformed.

Both surfaces are transformed to an object coordinate system while minimizing a goal function, which measures the sum of the squares of the Euclidean distances between them. The geometric relationships are established via 7-parameter similarity transformations. They can be replaced by another type if needed.

Each surface is associated with a set of 3D similarity transformation parameters,

$$\begin{bmatrix} x \\ y \\ z \end{bmatrix}_i = \begin{bmatrix} t_x \\ t_y \\ t_z \end{bmatrix}_i + m_i \mathbf{R}_i \begin{bmatrix} x_0 \\ y_0 \\ z_0 \end{bmatrix}_i \qquad (2)$$

where $\mathbf{R}_i = \mathbf{R}_i(\omega, \varphi, \kappa)$ is the orthogonal rotation matrix, $[t_x\ t_y\ t_z]_i^T$ is the translation vector, m_i is the uniform scale factor, and $(x_0, y_0, z_0)_i$ stand for the initial location of the surface.

Because Equations (1) are nonlinear, they are linearized by Taylor series expansion.

$$\begin{aligned} -e_i(x,y,z) &= g_j^0(x,y,z) + \frac{\partial g_j^0(x,y,z)}{\partial x_j} \mathrm{d}x_j + \frac{\partial g_j^0(x,y,z)}{\partial y_j} \mathrm{d}y_j \\ &+ \frac{\partial g_j^0(x,y,z)}{\partial z_j} \mathrm{d}z_j - g_i^0(x,y,z) - \frac{\partial g_i^0(x,y,z)}{\partial x_i} \mathrm{d}x_i \\ &- \frac{\partial g_i^0(x,y,z)}{\partial y_i} \mathrm{d}y_i - \frac{\partial g_i^0(x,y,z)}{\partial z_i} \mathrm{d}z_i \end{aligned} \qquad (3)$$

dx, dy and dz are the differentiations of the selected 3D transformation model in Equation (2):

$$\begin{aligned} \mathrm{d}x &= \mathrm{d}t_x + a_{10}\,\mathrm{d}m + a_{11}\,\mathrm{d}\omega + a_{12}\,\mathrm{d}\varphi + a_{13}\,\mathrm{d}\kappa \\ \mathrm{d}y &= \mathrm{d}t_y + a_{20}\,\mathrm{d}m + a_{21}\,\mathrm{d}\omega + a_{22}\,\mathrm{d}\varphi + a_{23}\,\mathrm{d}\kappa \\ \mathrm{d}z &= \mathrm{d}t_z + a_{30}\,\mathrm{d}m + a_{31}\,\mathrm{d}\omega + a_{32}\,\mathrm{d}\varphi + a_{33}\,\mathrm{d}\kappa \end{aligned} \qquad (4)$$

with a_{pq} as the coefficient terms.

Using the notation

$$g_x = \frac{\partial g^0(x,y,z)}{\partial x}, \quad g_y = \frac{\partial g^0(x,y,z)}{\partial y}, \quad g_z = \frac{\partial g^0(x,y,z)}{\partial z} \qquad (5)$$

and substituting Equations (4), Equation (3) results in:

$$\begin{aligned} -e_i(x,y,z) &= g_{xj}\,\mathrm{d}t_{xj} + g_{yj}\,\mathrm{d}t_{yj} + g_{zj}\,\mathrm{d}t_{zj} \\ &+ (g_{xj}a_{10} + g_{yj}a_{20} + g_{zj}a_{30})\,\mathrm{d}m_j \\ &+ (g_{xj}a_{11} + g_{yj}a_{21} + g_{zj}a_{31})\,\mathrm{d}\omega_j \\ &+ (g_{xj}a_{12} + g_{yj}a_{22} + g_{zj}a_{32})\,\mathrm{d}\varphi_j \\ &+ (g_{xj}a_{13} + g_{yj}a_{23} + g_{zj}a_{33})\,\mathrm{d}\kappa_j \\ &- g_{xi}\,\mathrm{d}t_{xi} - g_{yi}\,\mathrm{d}t_{yi} - g_{zi}\,\mathrm{d}t_{zi} \\ &- (g_{xi}b_{10} + g_{yi}b_{20} + g_{zi}b_{30})\,\mathrm{d}m_i \\ &- (g_{xi}b_{11} + g_{yi}b_{21} + g_{zi}b_{31})\,\mathrm{d}\omega_i \\ &- (g_{xi}b_{12} + g_{yi}b_{22} + g_{zi}b_{32})\,\mathrm{d}\varphi_i \\ &- (g_{xi}b_{13} + g_{yi}b_{23} + g_{zi}b_{33})\,\mathrm{d}\kappa_i \\ &- (g_i^0(x,y,z) - g_j^0(x,y,z)) \end{aligned} \qquad (6)$$

where a_{pq} and b_{pq} are the coefficient terms for the differentiation of the transformation equations of the i-th and j-th surface, respectively. The terms g_x, g_y and g_z are the numerical derivatives of the object surface function $g(x, y, z)$. They are defined as the elements of the local surface normal vectors at the exact surface correspondence locations (Gruen and Akca, 2005). The linearized observation Equations (6) are written for each element of the i-th surface.

Equations (6) result in the following linear systems in matrix/vector form

$$\begin{aligned} -\boldsymbol{e}_1 &= \mathbf{A}_1 \boldsymbol{x} - \boldsymbol{l}_1 \quad , \ \mathbf{P}_1 \\ -\boldsymbol{e}_2 &= \mathbf{A}_2 \boldsymbol{x} - \boldsymbol{l}_2 \quad , \ \mathbf{P}_2 \\ &\vdots \qquad\qquad \vdots \\ -\boldsymbol{e}_m &= \mathbf{A}_m \boldsymbol{x} - \boldsymbol{l}_m \quad , \ \mathbf{P}_m \end{aligned} \tag{7}$$

Equations (7) consist of m groups of observation equations. They can be combined in one sub-system as

$$-\boldsymbol{e} = \mathbf{A}\boldsymbol{x} - \boldsymbol{l} \quad , \ \mathbf{P} \tag{8}$$

where $\mathbf{A}$ is the design matrix, $\boldsymbol{x}$ is the parameter vector which contains n sets of transformation parameters, $\mathbf{P} = \mathbf{P}_{ll}$ is the a priori weight matrix, $\boldsymbol{l} = g_i^0(x, y, z) - g_j^0(x, y, z)$ is the discrepancies vector that consists of the Euclidean distances between the corresponding elements of the overlapping surfaces. The calculation of the discrepancy vector $\boldsymbol{l}$ and the numerical derivative terms g_x, g_y and g_z requires an appropriate correspondence search procedure (Akca and Gruen, 2005b).

Provided that $m \geq n$ is satisfied, the sub-system (of the design matrix) consisting of m Equations (7) implicitly contains the multiple overlap conditions. The normal equation matrix explicitly shows all the spatial relationships by non-zero off-diagonal elements (see Chapter 2.3.1).

With the statistical expectation operator $\mathrm{E}\{\ \}$, it is assumed that

$$\mathrm{E}\{\boldsymbol{e}\} = 0 \quad , \quad \mathrm{E}\{\boldsymbol{e}\boldsymbol{e}^{\mathrm{T}}\} = \sigma_0^2 \mathbf{P}_{ll}^{-1} \tag{9}$$

The parameters are introduced into the system as observables with the associated weight coefficient matrix $\mathbf{P}_b$ as

$$-\boldsymbol{e}_b = \mathbf{I}\boldsymbol{x} - \boldsymbol{l}_b \quad , \ \mathbf{P}_b \tag{10}$$

where $\mathbf{I}$ is the identity matrix and $\boldsymbol{l}_b$ is the (fictitious) observation vector. The weight matrix $\mathbf{P}_b$ has to be chosen appropriately, considering a priori information of the parameters.

2.2 The Generalized Model with Intensity Matching and Georeferencing

When some surfaces lack sufficient geometric information, their intensity information, if available, is introduced to the system. The intensity information is used to form quasisurfaces in addition to the actual ones. The formation of quasisurfaces is given in Akca and Gruen (2005a). The quasisurfaces are treated like actual surfaces in the estimation model. They contribute observation equations to the design matrix, joining the system by the same set of transformation parameters

$$-\boldsymbol{e}_c = \mathbf{A}_c \boldsymbol{x} - \boldsymbol{l}_c \quad , \ \mathbf{P}_c \tag{11}$$

where $\boldsymbol{e}_c$, $\mathbf{A}_c$ and $\mathbf{P}_c$ are the true error vector, the design matrix, and the associated weight coefficient matrix for the quasisurface observations, respectively, and $\boldsymbol{l}_c$ is the constant vector that contains the Euclidean distances between the corresponding quasisurface elements.

Reference points whose coordinates are defined in an external (object) coordinate system, which are imaged in additional intensity images, or can be located in the pointclouds, serve as the fourth type of observations. They are formulated as 3D similarity transformations from local pointcloud systems to the object coordinate system in linearized matrix form

$$-\boldsymbol{e}_d = \mathbf{A}_d \boldsymbol{x} - \boldsymbol{l}_d \quad , \ \mathbf{P}_d \tag{12}$$

where $\mathbf{A}_d$ is the design matrix, $\mathbf{P}_d$ is the associated weight matrix, and $\boldsymbol{l}_d$ is the discrepancies vector which contains the coordinate value differences of the reference points between the transformed local system and object coordinate system. At least 7 coordinate elements of 3 control points are needed for georeferencing.

Actually, the coordinates of the control points are not error-free quantities. In a strict model, they are treated as observations with their associated weight matrices as

$$-\boldsymbol{e}_e = \mathbf{A}_e \boldsymbol{x} - \boldsymbol{l}_e \quad , \ \mathbf{P}_e \tag{13}$$

where $\mathbf{A}_e$, $\boldsymbol{x}$, and $\mathbf{P}_e$ are the design matrix, the parameter vector, and the associated weight coefficient matrix for the observations of the control point coordinates, respectively, and $\boldsymbol{l}_e$ is the discrepancy vector that contains the differences between the observed and estimated coordinate values. Here, the vector $\boldsymbol{x}$ is extended to include the x-y-z coordinate values of the control points in addition to the transformation parameters.

Equations (12) eliminate the datum deficiency existing in Equations (8). Alternatively, the datum constraints can be imposed by fixing the minimal number of parameters in Equations (10).

The hybrid system of Equations (8), (10), (11), (12) and (13) is of the combined adjustment type that allows simultaneous matching of geometry and intensity and additionally georeferencing of multiple 3D surfaces. The Least Squares solution of the system gives the solution vector as

$$\begin{aligned} \hat{\boldsymbol{x}} = (&\mathbf{A}^{\mathrm{T}}\mathbf{P}\mathbf{A} + \mathbf{P}_b + \mathbf{A}_c^{\mathrm{T}}\mathbf{P}_c\mathbf{A}_c + \mathbf{A}_d^{\mathrm{T}}\mathbf{P}_d\mathbf{A}_d + \mathbf{A}_e^{\mathrm{T}}\mathbf{P}_e\mathbf{A}_e)^{-1} \\ &(\mathbf{A}^{\mathrm{T}}\mathbf{P}\boldsymbol{l} + \mathbf{P}_b\boldsymbol{l}_b + \mathbf{A}_c^{\mathrm{T}}\mathbf{P}_c\boldsymbol{l}_c + \mathbf{A}_d^{\mathrm{T}}\mathbf{P}_d\boldsymbol{l}_d + \mathbf{A}_e^{\mathrm{T}}\mathbf{P}_e\boldsymbol{l}_e) \end{aligned} \tag{14}$$

and the variance factor as

$$\hat{\sigma}_0^2 = \frac{\boldsymbol{v}^{\mathrm{T}}\mathbf{P}\boldsymbol{v} + \boldsymbol{v}_b^{\mathrm{T}}\mathbf{P}_b\boldsymbol{v}_b + \boldsymbol{v}_c^{\mathrm{T}}\mathbf{P}_c\boldsymbol{v}_c + \boldsymbol{v}_d^{\mathrm{T}}\mathbf{P}_d\boldsymbol{v}_d + \boldsymbol{v}_e^{\mathrm{T}}\mathbf{P}_e\boldsymbol{v}_e}{r} \tag{15}$$

where r is the system redundancy, $\boldsymbol{v}$, $\boldsymbol{v}_b$, $\boldsymbol{v}_c$, $\boldsymbol{v}_d$ and $\boldsymbol{v}_e$ are residual vectors for actual surface observations, parameter observations, quasisurface observations, reference point observations (for georeferencing) and control point coordinate observations, respectively.

The solution is iterative. At the end of each iteration all surfaces are transformed to their new states using the updated sets of transformation parameters, and the design matrices and discrepancy vectors are re-evaluated. The iteration stops if each element of the alteration vector in Equation (14) falls below a certain limit.

The estimation model is the Generalized Gauss-Markoff, which can accommodate any kind of functional constraint flexibly, e.g. concentric scans, certain rotational differences, parallel or perpendicular objects in the pointcloud data, etc.

2.3 Execution Aspects

2.3.1 Matrix Structures

Figure 1 shows the matrix structures of a hypothetical example of a data set with four pointclouds and three control points. For the sake of simplicity, the example does not cover the intensity matching case.

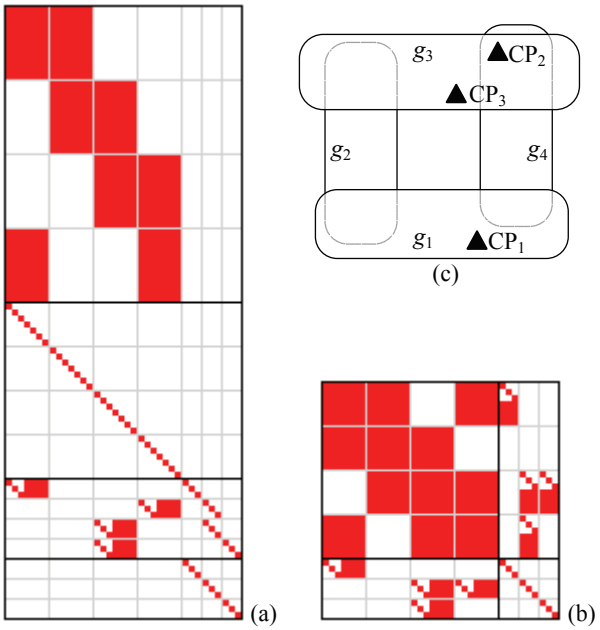

Figure 1. (a) The design matrix and (b) the corresponding normal equations matrix of a data configuration case (c) with four pointclouds and three control points.

The design matrix (Figure 1a) consists of 4 sub-systems. The first sub-system includes the observations of surface geometry. Each overlapping pointcloud, i.e. g_1-g_2, g_2-g_3, g_3-g_4 and g_4-g_1, gives a group of observation equations. The second sub-system represents the fictitious observations of the unknown transformation parameters. The third sub-system contains the reference point observations for the georeferencing. The last sub-system consists of the *x-y-z* coordinate value observations of the control points. The columns stand for 4 sets of transformation parameters (28 elements) and the coordinates of 3 full control points (9 elements).

The normal equations matrix comprises 4 sets of unknown transformation parameters and 3 sets of control point coordinates. The non-zero 7x7 sub-parts show the spatial overlaps among the pointclouds.

2.3.2 Memory Efficiency

In a typical real-world example, the data set may contain 10-20, sometimes more than 100 pointclouds. It is not operable to load all pointclouds into the physical memory. This most probably exceeds the memory limit of the computer. Our software implementation loads at maximum two pointclouds into the memory at any instant of (processing) time. All the information, e.g. 3D coordinates, correspondences, elements of the 3D boxing for the space partitioning, etc. are kept in the files whose contents are loaded into memory only when needed.

3. EXPERIMENTAL RESULTS

Because of the 125 anniversary of the construction of the Gotthard Tunnel (Switzerland), Credit Suisse has decided to have an exhibition in Zurich about the life and person of Alfred Escher (1819-1882), Swiss politician, promoter of the Gotthard Tunnel, railroad entrepreneur, and founder of Credit Suisse as well as of ETH Zurich.

In Zurich, there is a monument of Alfred Escher, which is located in front of the main railway station and is approximately 5 meter in high (9.5 meter considering also the basement). The goal of the project is the production of ten physical replicas of the Escher monument, starting from a 3D computer model.

The digitization was done with a Faro LS880 HE80 laser scanner, placed on a cherry picker (Figure 2). Totally 36 scans were acquired during two nights of on-site work. The data set contains approximately 4.4 million points with an average point spacing of 5-10 millimetres.

Figure 2. Pointcloud acquisition by laser scanning of the Alfread Escher statue on a cherry picker.

The proposed algorithm was used for the co-registration of the point clouds. Only the surface geometry and parameter observations were used. The example does not include the geo-referencing and intensity matching extensions.

At the first step, 3-5 tie points per pointcloud were interactively measured. Initial approximations were calculated by use of the tie point coordinates in a chained 3D similarity transformation. The first pointcloud was defined as the datum by fixing its parameters to a unit transformation with zero translation and rotation elements.

The transformation parameters of the all pointclouds were simultaneously calculated with sigma naught = 2.7 mm for the accuracy of the surface observations. Any surface correspondence whose Euclidean distance exceeds 6 times the current sigma naught value was excluded from the design matrix. The final iteration of the adjustment used 20,442,040 surface correspondences. A high noise level in the data slowed down the convergence to 16 iterations.

The computation lasted more than 18 hours processing time on a laptop computer with Intel dual-core 2.16 GHz CPU and 2 GB physical memory. The main reason is the file-access oriented design of our software implementation. The file access

for reading and writing is within a few milliseconds, while the memory access is within some nanoseconds. On the other hand, the memory request of the software has never exceeded 300 MB during the entire calculation.

Figure 3. The final 3D model of the Alfred Escher statue.

Figure 4. Still incomplete physical replica of the Alfred Escher monument (the missing parts are attached later).

After the co-registration step, all pointclouds were merged, filtered for noise reduction, sub-sampled and triangulated for surface generation. The 3D modelling operations were carried out using Geomagic Studio 9. Note that no editing has been made on the final model, except for the cropping of the area of interest (Figure 3). An edited version of the 3D model was used for the replica production. Ten replicas were produced at a scale 1:2 (Figure 4).

4. CONCLUSIONS

A method for the simultaneous co-registration of multiple 3D pointclouds is presented. It is capable of georeferencing as well as matching of the intensity information when some parts of the object surface lack sufficient geometry information. The estimation model is the Generalized Gauss-Markoff which allows any kind of object space conditions to be formulated as functional constraints, e.g. co-centric scans, perpendicular or parallel objects in the pointclouds, etc.

A practical experiment shows the capability of the method. A successful solution has been achieved. However, the computation time is the main burden. A more efficient software implementation and a multi-resolution approach during the iterations can accelerate the procedure substantially. The future work will also include experimentations with the georeferencing and intensity matching approaches.

5. REFERENCES

Ackermann, F., Ebner, H., and Klein, H., 1973. Block triangulation with independent models. Photogrammetric Engineering and Remote Sensing, 39 (9), 967-981.

Akca, D., Gruen, A., 2005a. A flexible mathematical model for matching of 3D surfaces and attributes. Videometrics VIII, Proc. of SPIE-IS&T Electronic Imaging, San Jose (California), USA, January 18-20. Proc. of SPIE, vol. 5665, pp.184-195.

Akca, D., Gruen, A., 2005b. Fast correspondence search for 3D surface matching. ISPRS Workshop Laser scanning 2005, Enschede, the Netherlands, September 12-14. International Archives of the Photogrammetry, Remote Sensing and Spatial Information Sciences, vol. XXXVI, part 3/W19, pp. 186-191.

Akca, D., Gruen, A., 2005c. Recent advances in least squares 3D surface matching. In: Gruen, A., Kahmen, H. (Eds.), Optical 3-D Measurement Techniques VII, Vienna, Austria, October 3-5, vol. II, pp. 197-206.

Al-Manasir, K., and Fraser, C.S., 2006. Registration of terrestrial laser scanner data using imagery. The Photogrammetric Record, 21 (115), 255-268.

Arun, K.S., Huang, T.S., Blostein, S.D., 1987. Least-squares fitting of two 3D point sets. IEEE Transactions on Pattern Analysis and Machine Intelligence, 9 (5), 698-700.

Beinat, A., and Crosilla, F., 2001. Generalized Procrustes analysis for size and shape 3D object reconstructions. Optical 3-D Measurement Techniques V, Vienna, October 1-4, pp. 345-353.

Benjemaa, R., and Schmitt, F., 1997. Fast global registration of 3D sampled surfaces using a multi-z-buffer technique. IEEE International Conference on 3D Imaging and Modeling, Ottawa, May 12-15, pp. 113-120.

Bergevin, R., Soucy, M., Gagnon, H., and Laurendeau, D., 1996. Towards a general multi-view registration technique. IEEE Transactions on Pattern Analysis and Machine Intelligence, 18 (5), 540-547.

Blais, G., and Levine, M.D., 1995. Registering multiview range data to create 3D computer objects. IEEE Transactions on Pattern Analysis and Machine Intelligence, 17 (8), 820-824.

Campbell, R.J., and Flynn, P.J., 2001. A survey of free-form object representation and recognition techniques. Computer Vision and Image Understanding, 81(2), 166-210.

Chen, Y., and Medioni, G., 1992. Object modelling by registration of multiple range images. Image and Vision Computing, 10 (3), 145-155.

Cunnington, S.J., and Stoddart, A.J., 1999. N-view point set registration: a comparison. British Machine Vision Conference, Nottingham, September 13-16, pp. 234-244.

Eggert, D.W., Fitzgibbon, A.W., and Fisher, R.B., 1998. Simultaneous registration of multiple range views for use in reverse engineering of CAD models. Computer Vision and Image Understanding, 69 (3), 253-272.

Greaves, T., 2005. Laser scanning shaves weeks from failure analysis of parking garage collapse. Spar ViewTM, 3(14), http://www.sparllc.com/archiveviewer.php?vol=03&num=14&file=vol03no14-01 (accessed August 2005).

Gruen, A., 1985. Adaptive least squares correlation: a powerful image matching technique. South African Journal of Photogrammetry, Remote Sensing and Cartography, 14 (3), 175-187.

Gruen, A., and Baltsavias, E., 1987. High-precision image matching for Digital Terrain Model generation. Photogrammetria, 42 (3), 97-112.

Gruen, A., Akca, D., 2005. Least squares 3D surface and curve matching. ISPRS Journal of Photogrammetry and Remote Sensing, 59 (3), 151-174.

Jokinen, O., and Haggren, H., 1998. Statistical analysis of two 3-D registration and modeling strategies. ISPRS Journal of Photogrammetry and Remote Sensing, 53 (6), 320-341.

Jokinen, O., 1998. Area-based matching for simultaneous registration of multiple 3-D profile maps. Computer Vision and Image Understanding, 71 (3), 431-447.

Krishnan, S., Lee, P.Y., Moore J.B., and Venkatasubramanian, S., 2005. Global registration of multiple 3D point sets via optimization-on-a-manifold. Eurographics Symposium on Geometry Processing, Vienna, July 4-6, pp. 187-197.

Lu, F., and Milios, E., 1997. Globally consistent range scan alignment for environment mapping. Autonomous Robots, 4 (4), 333-349.

Masuda, T., and Yokoya, N., 1995. A robust method for registration and segmentation of multiple range images. Computer Vision and Image Understanding, 61 (3), 295-307.

Neugebauer, P.J., 1997. Reconstruction of real-world objects via simultaneous registration and robust combination of multiple range images. International Journal of Shape Modeling, 3 (1-2), 71-90.

Pulli, K., 1999. Multiview registration for large data sets. IEEE International Conference on 3D Imaging and Modeling, Ottawa, October 4-8, pp. 160-168.

Schoenemann, P.H., and Carroll, R.M., 1970. Fitting one matrix to another under choice of a central dilation and a rigid motion. Psychometrika, 35 (2), 245-255.

Sharp, G.C., Lee, S.W., and Wehe, D.K., 2004. Multiview registration of 3D scenes by minimizing error between coordinate frames. IEEE Transactions on Pattern Analysis and Machine Intelligence, 26 (8), 1037-1050.

Stoddart, A.J., and Hilton, A., 1996. Registration of multiple point sets. IEEE International Conference on Pattern Recognition, Vienna, pp. B40- 44.

Sternberg, H., Kersten, Th., Jahn, I., and Kinzel, R., 2004. Terrestrial 3D laser scanning - data acquisition and object modeling for industrial as-built documentation and architectural applications. International Archives of the Photogrammetry, Remote Sensing and Spatial Information Sciences, 35(B7), 942-947, http://www.isprs.org/istanbul2004/comm5/papers/183.pdf (accessed August 2006).

Turk, G., and Levoy, M., 1994. Zippered polygon meshes from range images. In: A. Glassner (ed.), Proceedings of SIGGRAPH'94, Florida, July 24-29, pp. 311-318.

Williams, J.A., Bennamoun, M., Latham, S., 1999. Multiple view 3D registration: A review and a new technique. IEEE International Conference on Systems, Man, and Cybernetics, Tokyo, October 12-15, pp. 497-502.

Williams, J., and Bennamoun, M., 2001. Simultaneous registration of multiple corresponding point sets. Computer Vision and Image Understanding, 81 (1), 117-142.